Supersonic Combustion Studies for SCRamjet Engines

James F. Driscoll

Department of Aerospace Engineering, University of Michigan, Ann Arbor, MI 48109, USA jamesfd@umich.edu

In collaboration with: Chadwick C. Rasmussen, Kuang-Yu Hsu, Jeffrey M. Donbar, Mark R. Gruber, and Campbell D. Carter
Keywords: AJCPP, supersonic combustion, flame blowout

Abstract

Experiments were performed in order to examine the stability of hydrocarbon-fueled flames in cavity flameholders in supersonic airflows. Methane and ethylene were burned in two different cavity configurations having aft walls ramped at 22.5° and 90°. Air stagnation temperatures were 590 K at Mach 2 and 640 K at Mach 3. Lean blow out limits showed dependence on the air mass flowrates. Visual observations, planar laser induced fluorescence (PLIF) of nitric oxide (NO), and Schlieren imaging were used to investigate these phenomena. Large differences were noted between cavity floor and cavity ramp injection schemes. Cavity ramp injection provided better performance in most cases. Ethylene pilots have a wider range of stable operation than methane. Fuel flowrates at ignition showed similar trends as lean blowout limits, but higher flowrates were required.

Introduction

This research is one part of a NASA URETI funded program at both the University of Michigan and the University of Maryland. The propulsion goal that is addressed is to develop scaling laws and submodels which improve the capability of design codes to correctly predict flameholding, unsteady shock-flame interactions, dissociation losses to thrust, supersonic flame length, and regions of excessive wall heat transfer. Supersonic flames are operated in the Michigan Supersonic Flame Facility and at the Wright Patterson AFB Test Cell 19 supersonic combustion facility. Advanced laser flow visualization are being used to identify the physical processes associated with wall cavity flameholders, strut flameholders, shock-flame interactions, and local gas dissociation. Techniques include PLIF (planar laser induced fluorescence), imaging of the CH, OH, and NO radicals, and PIV (particle imaging velocimetry). Submodels for NASA codes are being developed that have the correct physics in order to provide accurate predictions of flame blowout. It also is planned to investigate engine dynamics, including engines dynamics, including vibrations due to thermal choking and acoustic resonance, unsteady loading, engine unstart, and shock wave oscillations.

Wall cavities have outstanding potential to serve as combined fuel injector/flameholders for scramjet combustors. The ability of cavity flameholders to stabilize hydrocarbon flames at flight Mach numbers between 4 and 6 recently has been confirmed [1]. A large amount of literature is available that characterizes various aspects of such devices [2-6]; however, a complete set of stability limits for cavity flameholders have not been made available in archival literature. In fact, few flame stability studies have been performed in supersonic environments for any geometry. Gruber et al. provide limited data on the operating range of cavity stabilized flames [7], Winterfeld looked at the stability of non-premixed hydrogen flames behind several coaxial baffle configurations [8,9], and Morrison et al. obtained very limited data for direct injection of propane into a supersonic flow [10].

The complexity of the flow field in a dual-mode scramjet combustor and the transient conditions associated with startup, where the flow field transitions from completely supersonic ($M\approx2$) to dual-mode, demand robust flameholding capabilities. Two main injection techniques have been identified: passive and direct [7]. With a passive injection scheme, fuel is injected into the air upstream of the cavity, in contrast to directly fueling the cavity. In the passive injection case, fuel enters the cavity only as a result of entrainment [11]. It has been shown that passive cavity fueling was insufficient over the range of operating conditions. As a result, direct fueling of a cavity pilot flame has been suggested and an extensive research effort is underway to optimize direct injection schemes [7]. This pilot would serve as a source of heat and combustion radicals for core flow combustion.

The use of a cavity as a combined fuel injector/flameholder for scramjet applications differentiates itself from traditional flameholders in several ways; most notably, direct injection of fuel into the recirculation zone creates a non-premixed environment where both mixing and combustion are occurring. Most of the previous literature has focused on flameholding in conditions where fuel and air are premixed [12,13]. In these studies the role of the recirculation zone is to provide combustion radicals and heat to ignite the incoming mixture [13].

Theoretical treatments of flame stabilization behind bluff bodies take into account the size of the recirculation zone, which changes as a result of blockage ratio, stoichiometry, and the presence of a flame [8]. Predominant features of the flow field over a cavity are illustrated in Fig. 1. Recirculation zone geometries in a cavity are constrained by the back wall, which suggests that mass and heat exchange between the cavity and the core flow depend upon the free shear layer spanning the cavity. The dynamics of this free shear layer are characterized primarily by the shape of the aft wall and the ratio of cavity length to depth (L/D).

Both the ramped and rectangular cavities are considered to be "open" in nature due to the fact that the shear layer reattaches at the aft wall rather than at the cavity floor for L/D $\leq$ 10 [3]. Consequently, entrainment into the cavity results from two phenomena: turbulent transport across the compressible shear layer and through the unsteady oscillations created by the shear layer interaction with the cavity aft wall. Cavities with a ramped aft wall have been shown to produce much smaller amplitude acoustic instabilities than those with a 90° aft wall [3,14]. However, computational studies have indicated that the presence of combustion may act to damp acoustic feedback mechanisms [5]. The effect of cavity geometry on flame stability has yet to be fully explored.

Empirical correlation parameters have been used to collapse blowout data for different flameholders as a function of stoichiometry. Ozawa included the effects of flameholder geometry by introducing a characteristic diameter. Combining this with the free stream temperature, pressure, and velocity, the lean blowout data for a variety of flameholders was condensed [15]. Huellmantel studied cavity flameholders and provided blowout data for subsonic flames stabilized in several different shapes of cavity [16]. Morrison was able to incorporate this data into Ozawa's correlation; however, extension of this correlation to the case of direct injection is challenging and has been attempted with limited results [9].

This study focuses on the blowout limits of a pilot flame fueled by direct injection into the cavity. It is argued that the results are general; i.e. they depend only on the local conditions (shape of the cavity, air and fuel flow properties, etc.) and not on the geometry of the entire combustor. Better understanding of the fundamental mechanisms of pilot flame stabilization will provide a much-needed foundation for design of scramjet combustors. In addition, the data presented herein will be useful for the modeling community in assessing design codes.

Experimental Setup

Experiments were performed in Test Cell 19 at the Propulsion Research Laboratory at Wright-Patterson Air Force Base in Dayton, OH. Details of the test facility can be found in the literature [17]. The half-tunnel configuration with a nozzle exit cross-section of 5.1 cm × 15.3 cm was used. A 17.8-cm-long constant area isolator is attached directly to the nozzle and is followed by a 74-cm-long ramp with one wall diverging at 2.5°. The cavities are mounted to the divergent wall. Two cavity geometries were tested as shown in Fig. 1. Both cavities were characterized by L/D=4, where the depth, D, was 1.7 cm, the width, W, was 15.3 cm, and the length, L, was defined as the cavity volume, V_{cav}, divided by $D \times W$. The aft wall of the ramped configuration is angled at 22.5° from the horizontal; the cavity with a 90° aft wall will be referred to as rectangular. Room-temperature fuel was injected into the cavity using two sets of injectors. The first set, which will be referred to as ramp injection (CR), was located on the cavity aft wall, 5 mm above the cavity floor as indicated in Fig. 1. Ten 1.6-mm-diameter injectors were spaced 1.3 cm apart. The floor injectors (CF) were located 5 mm downstream of the cavity leading edge. Four 1.6 mm diameter injectors were 2.5 cm apart. Ethylene and methane were chosen as fuels because they represent the limiting values for autoignition delay times and burning velocities of the components of cracked JP-7. Fuel flowrates were measured using Tylan mass flow controllers. Maximum fuel flowrates for the system were 5.8 g/s and 4.0 g/s for ethylene and methane respectively.

The set procedure was to flow air at 590 K for the Mach 2 cases and 640 K for the Mach 3 cases until

the entire apparatus reached a steady-state temperature. Wall temperatures in the cavity were 520-560 K. Air mass flowrate was varied by adjusting the plenum pressure upstream of the nozzle. Two spark plugs, located on the cavity floor, were activated and the fuel flowrate was increased until a flame was observed. A flame was stable if it could be sustained after the spark plugs were turned off. Fuel flowrate was adjusted slowly until blowout occurred. Instantaneous images of planar laser-induced fluorescence (PLIF) of nitric oxide (NO) were obtained to visualize the mixing in the cavity as a result of each injection scheme. A Lumonics Hyperdye dye laser was pumped with the second harmonic of an injection-seeded Spectra Physics Nd:YAG laser (GCR-170). The dye laser output was frequency-doubled using an Inrad Autotraker III and a second Autotraker III was employed where the doubled-dye beam was frequency-mixed with the residual IR beam from the Nd:YAG. The dye laser was set to a wavelength of 574 nm to produce frequency-mixed radiation at 226 nm to couple to the overlapped $Q_1(12)$ and $Q_2(20)$ transitions of the $A^2\Sigma^+ - X^2\Pi$ (0,0) band. A Princeton Instruments PIMAX CCD camera (with a 512 × 512 pixel array) with a UV lens was used to detect the fluorescence. Note that LIF images were not corrected for variations in line broadening, electronic quenching, or ground state population. See reference 10 for more detailed experimental information.

Results

Two global parameters of importance for a cavity flameholder are the fuel mass flowrate, m_f, and the characteristic air mass flowrate, m^*_A, which is defined as:

$$m^*_A = \rho_A U_A L W \qquad (1)$$

Stability of a flame in the cavity depends on the local air entrainment. It is useful to consider the global parameter m^*_A, which is proportional to area of contact between the cavity and the core flow ($L \times W$), since the exact rate of air entrainment into the cavity has not been determined experimentally. For comparison to future computations, the present study focused on measurements of m_f and m^*_A at blowout. To explain the measured blowout limits, some images of fuel concentration fields are presented.

(1) Effects of Fuel Injector Location

One concept that was assessed is whether the cavity recirculation zone can be modeled as a well-stirred reactor. If well-mixed conditions do exist, only the total amount of fuel and air entering the cavity are relevant and the location where fuel is injected should not be important. Figure 2 shows that for the Mach 2 airflow, the location of the fuel injector has a major effect on the lean blowout (LBO) limits. Consider curves A and F in Fig. 2. Curve A represents the best case since it is the lowest curve (least amount of fuel required) and it corresponds to CR injection of ethylene fuel. Curve F is much higher than curve A; curve F represents the same conditions as A except that that fuel injection was from the CF location. It is concluded that the location of fuel injection (with respect to the recirculation zone) is important and that well-stirred conditions are not occurring.

One reason for the differences caused by the location of fuel injection is suggested by Fig. 3. This is a Schlieren image of the fuel jet issuing from the CF injectors while combustion is taking place. The fuel jet (indicated with a white arrow) is seen to issue vertically upward and it provides fuel to the shear layer but not directly to the recirculation zone, since no fuel is seen within the cavity downstream of the jet. Previous studies have shown that the main recirculation zone does not extend to the upstream portion of the cavity. Instead, a small secondary recirculation zone exists, as shown in Fig.1. Thus with CF injection, it is observed that fuel does not directly enter the main recirculation zone. The fuel is forced to enter directly into the main recirculation zone in the case of CR injection.

Figs. 4 and 5 are PLIF images of fuel concentration in a non-reacting cavity and indicate that downstream injection provides superior fuel-air mixing. Trace amounts of NO were added to the fuel. The fuel concentration is very uniform in Fig. 4 (CR injection) but is non-uniform in Fig. 5 (CF injection) since the fuel is deposited in the shear layer and not the recirculation zone. This result is consistent with subsonic, trapped vortex studies [18, 19], which also show that the relative locations of the fuel injector and the main recirculation zone are important to flame stability.

This explanation is further corroborated by direct photographs of the flame chemiluminescence, shown in Figs. 6 and 7. In Fig. 6, CR injection is used and the flame extends deeper into the cavity. The flame in Fig. 7 (CF injection) does not extend to the bottom of the cavity but has a long thin zone near the top of the cavity where the shear layer exists. The combustion deep in the cavity, rather than in the shear layer, explains the improved stability offered by CR injectors. In general, LBO

data was more scattered for the case of CF injection than for CR injection. Data points corresponding to curve F are averaged values of the tests performed at each air flowrate. The standard deviation was approximately 15% of the mean at each value of m^*_A for this case. Scatter in the data can be attributed to the unsteady fueling of the cavity as a result of the non-uniform fuel distribution observed in Fig. 5.

Tests were performed to see if some optimum conditions would occur if both the CR and CF fuel injectors were used simultaneously. Figure 8 shows the lean limit as the relative fuel flowrates from the two injectors were varied. The results fall on a straight line for each of the two air flowrates considered. This indicates that there is a monotonic variation between the better CR injection and the less-desirable CF injection, and there exists no optimum when both are used.

(2) Effect of Fuel Type, Mach Number

Ethylene flames were always more stable than methane flames, as illustrated by curves D and E in Fig. 2. Curve D (ethylene) lies below curve E (methane) for the same conditions (Mach 2, CR injection, rectangular cavity). This trend is similar for the other conditions; for CR injection, curve A (ethylene) also is lower than curve B (methane). This difference is expected since the ignition delay time is much shorter for ethylene than for methane. The maximum laminar flame speed of ethylene (73 cm/s) also exceeds that of methane (43 cm/s).

Figure 9 shows the lean limits for ethylene flames when the Mach number was increased from 2 to 3. A comparison of Fig. 2 and Fig. 9 indicates that the lean limits did not change significantly between the two cases. Curves G and A are similar, as are curves H and D and curves J and F. In each case the first curve was obtained at Mach 3 and the second at Mach 2. While increasing the Mach number tends to reduce the static pressure, the corresponding value of m^*_A is similar for both cases because m^*_A is proportional to the density of the air.

Comparing the ramped cavity shape to the rectangular cavity, there is no clear evidence that the blowout limits of one cavity shape are superior to the other for all conditions. The rectangular cavity performed better if CF injection is used (curve C in Fig. 2 lies below curve F). However, the ramped cavity performed better when the CR injector was used (curve A lies below curve D in Fig. 2). It has been hypothesized that an optimum ramp angle could improve flame stability. This angle controls the location where the shear layer impinges on the cavity rear wall, which affects the strength of the recirculation zone, the air entrainment rate, shock wave locations and stagnation pressure losses. More pronounced shear layer oscillations are expected in the case of the rectangular cavity, which leads to greater entrainment near the aft wall. Since CF injection has been observed to fuel the shear layer, entrainment from the unsteady shear layer interaction with the aft wall is required to recirculate fuel and hot products into the cavity. As a result, the combination of CF injection into the rectangular cavity resulted in better stability than CF injection into the ramped cavity.

(3) Rich Blowout Limits

The rich blowout (RBO) limits for the present configuration are given in Fig. 10. It was found that the CF injectors performed better in all cases at the rich limits than the CR injectors, which is opposite to the LBO trends. For example, curve M (CF injection) lies above curve N (CR injection), and the higher curve represents improved stability at the rich limit. Curves K and L (CR injection) appear to be the most stable (highest) curves in Fig. 10, but CF injection for these conditions yielded flames so stable that fuel flowrates exceeded 5.8 g/s, which was the maximum measurable ethylene flowrate.

The rich limits can be explained by the same argument used for the lean limits. The CF injectors create the vertical jet seen in Fig. 3. Thus, the fuel enters the shear layer where excess air is available and fuel is allowed to escape or bypass the cavity without reacting. The CR injectors inject so much fuel directly into the recirculation zone that it becomes flooded and not flammable. Again these finding are consistent with trapped vortex ideas [18,19]; the location of the injector with respect to the recirculation zone is important.

As expected, the methane flames were not as stable as the ethylene flames at the rich limit; curves O and P in Fig. 10 correspond to methane and lie far below the other curves. The effect of Mach number on the rich limits is significant, whereas Mach number had little effect on the lean limits. Curve K (Mach 2) and curve N (Mach 3) have all other conditions matched, and it is apparent that flames in a Mach 2 flow are much more stable near the rich limit than in a Mach 3 case. To explain these differences, detailed simulations are needed to account for the changes in static pressure and

temperature on the chemistry along with decreased characteristic flow times as the Mach number is increased. Note that the rich limit of the pilot flames differs from the rich limit of the entire combustor, which occurs when too much fuel is injected into the air upstream of the cavity.

(4) Ignition Limits

A quantity of importance is the ignition limit; i.e. the minimum fuel flowrate that results in cavity flame ignition. This number differs from the lean limit because at LBO the cavity recirculation zone contains hot products, while at ignition the recirculation zone is cold. As illustrated in Fig. 11, values of m_f through the CR injectors at ignition are approximately 1.5 times higher than at LBO in the ramped cavity. In the rectangular cavity, ignition limits occur at nearly 3 times higher fuel flowrates than LBO. Figure 12 shows ignition limits for CF injection. Some scatter in the ignition data can be attributed to wall temperatures in the cavity. Flames could not even be established for some cases unless the walls were adequately heated prior to fuel injection. This behavior was particularly apparent in some cases at Mach 3 with low m^*_A. Specification of fuel flowrates necessary for ignition requires specific attention when designing a cavity fuel injector/flameholder. It is important to note that the static temperatures in this experiment are much lower than expected in a flight condition.

(5) Analysis to Explain the Measured Flame Blowout Limits

Figure 13 shows the basic physics of the present problem. At the top of the figure one sees that a step, a cavity and a strut all create a shear layer that exists between the outer air stream and a recirculation zone. Three possible fuel injection locations are shown: upstream of the step, such that fuel goes directly into the shear layer (a), or into the upstream (b) or downstream region (c) of the recirculation zone. The location of the fuel injector is an important new variable that does not appear in previous analyses of premixed flame blowout limits. It is expected that if fuel is injected directly into the recirculation zone (Fig. 13c) then excessive fuel injection could easily "flood" the cavity with a fuel-rich mixture, forcing the flammable region to move upward and into the high-speed airstream. This would tend to limit the fuel-rich operation. However, if fuel is injected upstream of the step (Fig. 13a), the goal is to entrain a sufficient amount of fuel into the cavity so that the flammable zone overlaps the low velocity zone in the cavity. Thus, upstream injection may limit the fuel-lean operation of the flameholder.

The analysis applies to the geometry shown in Fig. 13; a shear layer exists between a high-speed airstream and a recirculation zone. Fuel may be injected directly into the recirculation zone, but air is not injected; air can enter the recirculation zone only by first being entrained into the shear layer. Thus the analysis applies to nearly all of the nonpremixed flames reported in the literature that are stabilized by bluff-bodies, cavities and by swirl. The following five assumptions are made.

The first assumption is that upstream of a lifted flame base, there exists a flammable zone (between the fuel-rich and fuel-lean regions) in which the reactants become mixed and a stoichiometric contour exists. Along the upper and lower sides of the flammable zone seen in Fig. 13a the equivalence ratio is approximately 0.5 and 2.0, respectively.

The fundamental assumption for flame stability is that even though the fuel and air initially are nonpremixed, the flame base is a premixed flame that propagates along the stoichiometric contour at a velocity (S_{base}) that is equal to the local gas velocity (U_{gas}). S_{base} is a function of the temperature (T_s) of the reactants just upstream of the flame base, and the reactants are heated by heat transfer from the recirculation zone.

$$S_{base}(T_s) = U_{gas} \qquad (2)$$

Another requirement for stability is that:

$$d(S_{base})/dx > d(U_{gas})dx. \qquad (3)$$

This requirement ensures that if the flame is perturbed downstream, at the new location the propagation speed will exceed the local gas velocity, so the flame will propagate back to its original location.

Blowout is defined to occur when the flame liftoff distance (h) equals the length of the recirculation zone; that is when:

$$h = L_{RZ} \qquad (4)$$

The gas upstream of the flame base is heated by heat transfer from the recirculation zone, and this no longer occurs when h exceeds L_{RZ}.

It is assumed that the flame base is always located within the stratified shear layer (shown in Fig. 13)

and not within the recirculation zone. There is experimental evidence to justify this assumption. The stoichiometric fuel-air ratio for hydrocarbon (and for hydrogen) fuel does not exceed 0.10, thus the stoichiometric contour if forced to be much closer to the air stream (where the local fuel-air ratio is zero) than to any fuel-rich region, where the fuel-air ratio is infinite. Near the fuel-rich blowout limit, measurements have shown that the recirculation zone is filled with hot products and fuel, but contains essentially no oxygen. Near the lean blowout limit, it is assumed that the recirculation zone contains products and entrained air, but no fuel.

In the shear layer, it is assumed that the profiles of mixture fraction, stagnation temperature, and ρu vary linearly in the transverse (y) direction between the airstream boundary conditions, which are known, and the boundary conditions at the lower edge of the shear layer, which are not known. In compressible shear layers, these assumptions are consistent with measurements. In the recirculation zone, it is assumed that there is a uniform temperature and a uniform mixture of either fuel and products or air and products.

Based on the above five assumptions, the problem reduces to that of a flame that is stabilized in a stratified premixed shear layer. The boundary conditions on the air side are uniform and known (velocity = U_A, temperature = T_A and mixture fraction f = 0). On the fuel side of the shear layer, the boundary conditions are complicated. We choose to define the lower edge of the shear layer as the location where the axial velocity is zero. Thus the lower part of the shear layer overlaps the upper portion of the recirculation zone. At this lower edge, T_2 and f_2 depend on the ratio of fuel to products in the recirculation zone, and U_2 is zero by definition.

The above five assumptions are not the same as those that often have been applied to the different problem of flame blowout when the reactants are initially premixed. For the initially premixed case it has been assumed that the chemical reactions occur within the recirculation zone, which is assumed to be a "distributed reaction zone" and thus a "flame" does not exist. Instead of requiring a flame speed to match a gas velocity previous work has assumed that the chemical time of the distributed reaction must equal a characteristic flow time, which is the length of the recirculation zone divided by the air flow velocity.

It is now possible to describe a physical explanation of flame blowout that is based on the above four assumptions. Figure 14a provides a schematic curve (labeled U_{gas} for U_{A1}) that represents the gas velocity along the stoichiometric contour in the shear layer when the air velocity is set to the value U_{A1}. This gas velocity is seen to decrease in the x direction until it crosses over the value of S_{base}, which is the propagation speed of the flame base. The x-location where U_{gas} equals S_{base} is the liftoff height h_1. As the air velocity is increased to U_{A2}, Fig. 14a shows that the entire curve of U_{gas} moves to the right, which increases the liftoff distance. However, the propagation speed curve (S_{base}) drops to nearly zero at the end of the recirculation zone, where the gas in the shear layer is no longer heated by heat diffusing from the recirculation zone. At the air velocity U_{A3}, Fig. 2a shows that blowout has occurred.

Now consider Fig. 14b. In this case the air velocity is held constant, so only one curve of U_{gas} is shown. As the fuel velocity is increased to the rich blowout limit, the mixture of fuel and products in the recirculation zone become cooler, which causes the propagation speed S_{base} to decrease as shown. The liftoff distance increases until it exceeds L_{RZ} and blowout occurs.

To use our fundamental flame stability criterion (Eq.2) it is necessary to estimate the two parameters that appear in Eq. 2: the gas velocity U_{gas} and the temperature T_s just upstream of the flame base. Before considering the stratified shear layer discussed above, first consider a simple lifted jet flame. Previously, it has been noted that:

$$U_{gas} = U_F f_s \beta \qquad (5)$$

The gas velocity along the stoichiometric contour should be $U_F f_s$ if there is no disturbance caused by the flame and β is a factor that accounts for gas expansion due to the flame. This follows from the similarity between the equations for the mixture fraction field and the velocity field, which indicates that u/U_F should equal f everywhere. Along the stoichiometric contour $f = f_s$ and $u = U_{gas}$. However, the presence of an "edge" flame causes a divergence of the streamlines, causing the factor β to be $c_1 (\delta/x)$ where c_1 is a constant and δ is the flame thickness α/S_L. For the simple jet flame problem, we set the value of x in Eq. 10 to h, we set the temperature of the reactants T_s in Eq. 2 to 300 K, and combine Eqs. 2 and 5 to obtain:

$$h = c_1 U_F f_s / (S_L^2/\alpha) \quad (6)$$

This is the well-known relation for the liftoff height of a jet flame. The blowout limit of a jet flame is determined by the criterion that the liftoff height cannot exceed the length of the flammable zone of the jet; this length is known to be $c_2 d / f_s$ where d is the jet diameter. Equating this to the liftoff height given by Eq. 6, one obtains a blowout velocity of:

$$U_F = d (S_L^2/\alpha) (c_2/c_1) f_s^{-2} \quad (7)$$

which has been verified by experiment.

Now consider the stratified shear layer shown in Fig. 14a. The lower edge of the layer is defined as the location where u =0. Based on the assumption above, ρu varies linearly from $\rho_A U_A$ at the upper edge to zero at the lower edge, and that mixture fraction f varies from zero at the upper edge to a value of f_2 at the lower edge. It follows that the y-location where f equals f_s can be computed and the value of $\rho_s U_{gas}$ at this y-location is:

$$\rho_s U_{gas} = \rho_A U_A (1 - f_s/f_2) \beta \quad (8)$$

where β is a factor that accounts for gas expansion by the presence of the flame. For simplicity, we assume that β has the same value as for a jet flame ($c_1\delta/x$) and δ is α/S_{base}. Combining Eqs. 7 and 2 and setting x = h

$$S_{base}(T_s) = U_A (\rho_A/\rho_s) (1 - f_s/f_2) (c_1 \alpha/S_{base}) /h \quad (9)$$

After applying our blowout criterion that $h = L_{RZ}$, rearrangement yields a relation for the required step height H to stabilize the flame:

$$(H/U_A)/(\alpha_0/S_0^2) = (H/L_{RZ})[S_{base}/S_0)]^{-2}[\alpha/\alpha_0] (\rho_s/\rho_A) (1 - f_s/f_2) c_1 \quad (10)$$

where the term (H/L_{RZ}) can realistically be set to 0.5, and S_0 and α_0 are the reference values of the stoichiometric laminar burning velocity and thermal diffusivity at 300 K and 1 atm.

Therefore a Damkohler number appears on the left side of Eq. 10, and the right side is a function of the temperature (T_s) on the stoichiometric contour just upstream of the flame base. To estimate the temperature T_s, the above assumption is applied. The stagnation temperature profile across the shear layer varies linearly between the known value T_{0A} at the outer edge to the recirculation zone value T_{RZ} at the lower edge. From linear interpolation, it follows that at the y-location where the mixture fraction is stoichiometric, can be computed and the local stagnation temperature is:

$$T_{0s} = T_s = T_{0A} + (f_s/f_2) (T_{RZ} - T_{0A}) \quad (11)$$

Because of the flame, the flow is decelerated near the flamefront, so it will be assumed that T_s is equal to T_{0s}. The temperature in the recirculation zone (T_{RZ}) depends on the mass fraction of products $Y_{P,RZ}$, which coexist with fuel only near the rich limit, and with air only near the lean limit, so:

$$T_{RZ} = Y_{P,RZ} T_{AD} + (1 - Y_{P,RZ}) T_F \quad \text{rich} \quad (12a)$$
$$T_{RZ} = Y_{P,RZ} T_{AD} + (1 - Y_{P,RZ}) T_{0A} \quad \text{lean} \quad (12b)$$

Combining Eqs. 11 and12 yields:

$$T_s = T_{0A} + (f_s/f_2) [Y_{P,RZ} (T_{AD} - T_F) + (T_F - T_{0A})] \quad \text{rich limit} \quad (13a)$$
$$T_s = T_{0A} + (f_s/f_2) [Y_{P,RZ} (T_{AD} - T_{0A})] \quad \text{lean limit} \quad (13a)$$

The problem has now been reduced to that of determining the mass fraction of products in the recirculation zone ($Y_{P,RZ}$). The adiabatic flame temperature (T_{AD}) and initial fuel and air temperatures (T_F, T_{0A}) in Eq. 13 are given. If one considers the flame shown in Fig. 14a, it is clear that there is a total mass flowrate of products created by the flame (m_P), and the portion of this flowrate that enters the recirculation zone is $m_{P,RZ}$. Similarly, the total mass flowrate of fuel injected is $m_{F,RZ}$, and the portion of this that enters the recirculation zone under rich conditions is $m_{F,RZ}$. Therefore:

$$Y_{P,RZ} = m_{P,RZ} / (m_{P,RZ} + m_{F,RZ}) \quad \text{rich} \quad (14a)$$
$$Y_{P,RZ} = m_{P,RZ} / (m_{P,RZ} + m_{A,RZ}) \quad \text{lean} \quad (14b)$$

We now define four entrainment parameters:

$$\varepsilon_1 = m_{P,RZ} / m_P \qquad \varepsilon_2 = m_{F,RZ} / m_F \quad (15a)$$
$$\varepsilon_3 = m_{A,RZ} / m_{A,SH} \qquad \varepsilon_4 = m_{F,SH} / m_F \quad (15b)$$

The quantity $m_{F,SH}$ in Eq. 15b is the portion of the total fuel mass flow rate that enters the shear layer when the lean blowout limit is approached. The mass flow of air entrained into the shear layer ($m_{A,SH}$) is $\rho_A U_A \delta_A W$, where δ_A is the shear layer thickness (from y = 0 to the upper edge of the layer at the axial location at the end of the recirculation zone). Since d δ/dx is typically 0.09, it follows that δ_A is 0.09 L_{RZ},

$$m_{A,SH} = \rho_A U_A 0.09 L_{RZ} W \quad (16)$$

and we define the characteristic air mass flowrate (m_A^{**}) to be:

$$m_A^{**} = 0.01\,\rho_A\,U_A\,H\,W = m_{A,SH}\,(0.01/0.09)\,(H/L_{RZ}) \qquad (17)$$

Conservation of mass requires that m_P equal ($m_{F,SH} + m_{A,SH}$) and the stoichiometric fuel-air ratio (r_s) is ($m_{F,SH}/m_{A,SH}$) so it follows that:

$$m_P = m_{A,SH}\,(1 + r_s) \quad \text{rich limit} \qquad (18a)$$
$$m_P = m_{F,SH}\,(1 + r_s^{-1}) \quad \text{lean limit} \qquad (18b)$$

Combining Eqs. 14-28 yields:

$$Y_{P,RZ} = [\,1 + (\varepsilon_1/\varepsilon_2)\,(0.01/0.09)\,(1 + r_s)^{-1}\,(H/L_{RZ})\,(m_F/m_A^{**})]^{-1} \quad \text{rich limit} \qquad (19a)$$
$$Y_{P,RZ} = [1 + (\varepsilon_3/(\varepsilon_1\varepsilon_4))\,(0.09/0.01)\,(1 + r_s^{-1})^{-1}\,(L_{RZ}/H)\,(m_F/m_A^{**})^{-1}]^{-1} \quad \text{lean} \qquad (19b)$$

Note that Eqs. 19a and 19b display the correct trends. As the mass flowrate of fuel (m_F) is increased near the rich limit, Eq. 24a indicates that the mass fraction of hot products decreases, leading to a cooler recirculation zone, and less heating of the reactants ahead of the flame, leading to blowout. However, as the mass flowrate of fuel is increased near the lean limit, Eq. 19b indicates that more hot products will be formed and the flame becomes more stable.

One other quantity required in Eq. 10 is the mixture fraction f_2 at the lower edge of the shear layer. The mixture in the recirculation zone is assumed to be uniform in space and there exists a linear equilibrium state relation between mixture fraction and gas temperature, which is:

$$f = 1 - (1\text{-}f_s)\,(T - T_F)/(T_{AD} - T_F) \quad \text{rich} \qquad (20a)$$
$$f = f_s\,(T - T_A)/(T_{AD} - T_A) \quad \text{lean} \qquad (20b)$$

Eq. 20a indicates that for pure fuel ($T = T_F$) f is 1, and Eq. 20b indicates that for pure air ($T = T_A$) f is 0. For both relations, when $T = T_{AD}$, f equals f_s. Using the state relations (Eqs. 20) we replace T with the value of T_{RZ} given by Eq. 12, and set f in Eqs. 20 to f_2, which yields:

$$f_2 = 1 - (1\text{-}f_s)\,Y_{P,RZ} \quad \text{rich limit} \qquad (21a)$$
$$f_2 = f_s\,Y_{P,RZ} \quad \text{lean limit} \qquad (21a)$$

The result of the scaling analysis

The required step height H to avoid blowout was given by Eq. 10:

$$(H/U_A)/(\alpha_0/S_0^2) = (H/L_{RZ})\,[S_{base}/S_0)]^{-2}\,[\alpha/\alpha_0]\,(\rho_s/\rho_A)\,(1 - f_s/f_2)\,c_1 \qquad (10)$$

where:
$$S_{base}/S_0 = (T_s/300K)^2 \qquad (22)$$
$$\alpha/\alpha_0 = (T_s/300K)^{1.5}\,(p/1\ atm)^{-1} \qquad (23)$$
$$H/L_{RZ} = 0.5 \qquad (24)$$

The above four equations, combined with previous equations for Ts and f2 (Eqs. 13, 19, 21) yield a set of relations that predict rich blowout and lean blowout limits. At this point, these relations give the correct measured trends. Additional measurements and comparisons are being made to determine if these provide general scaling relations for the rich limit and one for the lean limit that can be used by engine designers.

Conclusions

Stability limits were obtained for cavity stabilized flames in supersonic flows and the effects of injector location have been studied to gain insight into the blowout mechanisms in directly fueled cavity injector/flameholders. Several general conclusions have been reached based upon the data.

1. Flame blowout limits were highly dependent upon the air flowrate, injection location, fuel type, and cavity geometry. Thus, well-stirred reactor concepts are not applicable to cavity injector/flameholders with direct fuel injection.

2. Fuel injection from the aft wall (CR injection) provided better flame stability at the lean limit, while fuel injection from the floor location (CF injection) provided better stability at the rich limit. Both findings are explained by flow visualization that shows that the CF injection allows a large amount of fuel to escape the cavity through the shear layer, resulting in localized fuel pockets and incomplete mixing. Injection from the ramp leads to longer residence times and more uniform mixing and combustion.

3. Ethylene flames were stable over a wider range of fuel flowrates than methane flames, as expected because of the shorter ignition delay time of ethylene. Methane flames would not ignite in a Mach 3 airflow due to the low static temperature and pressure.

4. Lean limits for ethylene in the Mach 2 and Mach 3 cases were comparable, although flames were stabilized over a smaller range of m^*_A in the Mach 3 air flow.

5. Fuel flowrates required for ignition of the flame were greater than flowrates at LBO, but showed similar dependence upon air entrainment. Ignition also demonstrated a high degree of dependence upon cavity wall temperature.

6. An analysis is presented which does predict the observed experimental trends in the rich and lean blowout limits.

Acknowledgments
Support provided by NASA for the URETI Reusable Launch Vehicle Center. This work was made possible by the Air Force Office of Scientific Research, monitored by Dr. Julian Tishkoff.

References

[1] T. Mathur, et al., *J. Prop. Power*, 17(6)(2001).

[2] J.M. Donbar, et al., *Proc. Combust. Inst.* 28(2000)679-687.

[3] M.R. Gruber, R.A. Baurle, T. Mathur, and K.-Y. Hsu, *J. Prop. Power*, 17(1)(2001).

[4] K.H. Yu, K.J. Wilson, and K.C. Schadow *J. Prop. Power*, 17(6)(2001).

[5] D.L. Davis and R.D.W. Bowersox, AIAA Paper 97-3270, Amer. Inst. of Aero. Astro., 1997.

[6] A. Ben-Yakar and R.K. Hanson, *J. Prop. Power*, 17(4)(2001).

[7] M.R. Gruber, J.M. Donbar, C.D. Carter, and K.-Y. Hsu, *Proc. Intl. Soc. Air-Breathing Engines*, Report ISABE 2003-1204, 2003.

[8] G. Winterfeld, *Proc. Combust. Inst.* 10(1965)1265-1275.

[9] G. Winterfeld, *Cranfield International Propulsion Symposium on Combustion in Advanced Gas Turbine Systems* 1967.

[10] C.Q. Morrison, R.L. Campbell, and R.B. Edelman, *Proc. Intl. Soc. Air-Breathing Engines*, Report ISABE 97-7053, 1997.

[11] K.-Y. Hsu et al., AIAA Paper 2000-3585, Amer. Inst. of Aeronaut. and Astronaut., 2000.

[12] S.L. Plee and A.M. Mellor, *Combust. Flame*, 35:61-79 (1979).

[13] E.Z. Zukoski and F.E. Marble, *Gas Dynamics Symp. on Aerothermy*, Northwest. U., 1956.

[14] X. Zhang, A. Rona, and J.A. Edwards, *Aeron. Journal*, 102, March 1998, pp. 129-136.

[15] R.I. Ozawa, Technical Report AFAPL-TR-70-81, (1971).

[16] L.W. Huellmantel, R.W. Ziemer, and A.B. Cambel, *Jet Propulsion*, (1957) pp.31-43.

[17] M.R. Gruber and A.S. Nejad, *J. Prop. Power*, 11(5)(1995).

[18] K.-Y. Hsu, L.P. Goss. and W.M. Roquemore, *J. Prop. Power*, 14(1)(1998).

[19] V.R. Katta and W.M. Roquemore, *J. Prop. Power*, 14(3)(1998).

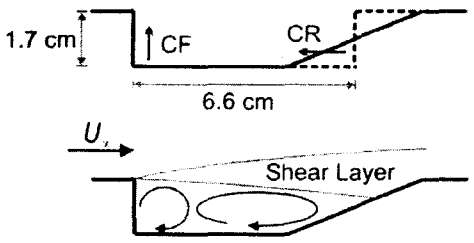

Figure 1: The top picture shows the cavity geometry for the ramped (solid line) and rectangular (dashed line) geometries. Injection locations are also marked as cavity ramp (CR) and cavity floor (CF). Below is a schematic illustrating the main flow features including the free shear layer and the two recirculation zones predicted from 2D computational studies [3].

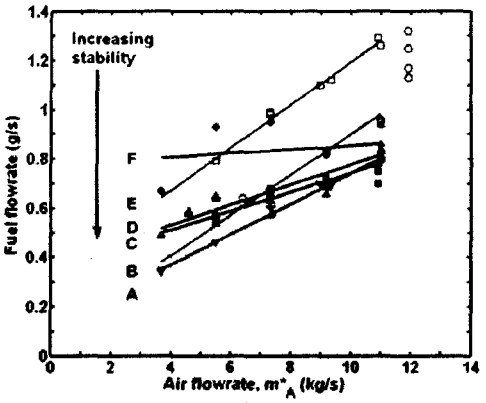

Figure 2: Lean blowout (LBO) limits at Mach 2. Best stability (curve A) was achieved with CR fuel injection. Reduced stability (curve F) occurred with CF injection. Methane flames (curve E) were less stable than ethylene flames (curve D). Data corresponds to curves as follows: A) ▼, ethylene, CR injection, ramped cavity; B) O, methane, CR injection, ramped cavity; C) ■, ethylene, CF injection, rectangular cavity; D) ▲, ethylene, CR injection, rectangular cavity; E) □, methane, CR injection, rectangular cavity; F) ●, ethylene, CF injection, ramped cavity.

Figure 3: Schlieren image of reacting cavity with injection of ethylene from the cavity floor (CF). High-speed Schlieren movies show that the shear layer interaction with the aft ramp is unsteady, but a large amount of fluid from the shear layer appears to flow directly out of the cavity over the ramp. Also visible is the chemiluminescence from the flame.

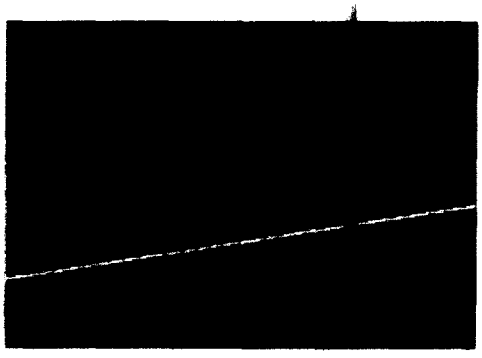

Figure 4: Half-span image of the fuel mixing pattern using NO PLIF. Air seeded with NO was injected into a non-reacting cavity via CR injectors. The image plane is approximately 77 mm wide (half of the cavity width) and is located 12.7 mm from the leading edge of the cavity. The flow direction is out of the page,

the left side of the image corresponds to the wall of the test section, and the right wall to the centerline of the combustor. The white line represents the floor of the cavity and the cavity height is approximately the height of the NO layer. This illustrates the fairly uniform distribution of fuel within the cavity when CR injection is used.

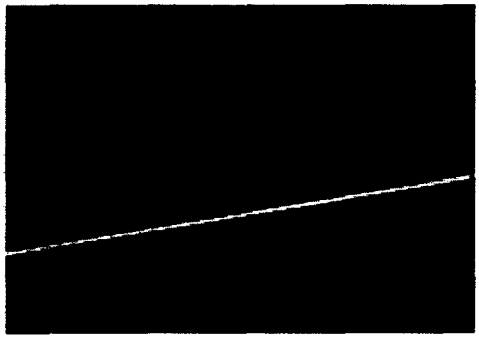

Figure 5: The above image is for the same conditions as Figure 4 except CF injection is used. CF injection leads to the formation of localized zones of fuel in the shear layer region and non-uniform fuel distribution.

Figure 6: Flames fueled with CR injection at moderate flowrates, such as the one in the above image, filled a large portion of the cavity upstream of the injection location. This image shows the full span and the air is flowing from left to right. Reaction appears to take place deep in the cavity as well as in the shear layer.

Figure 7: This image shows chemiluminescence of a flame fueled by CF injectors. Most of the reaction appears to be taking place in the shear layer and upstream near the leading edge of the cavity. Very little reaction appears deep within the cavity, in contrast to Figure 6.

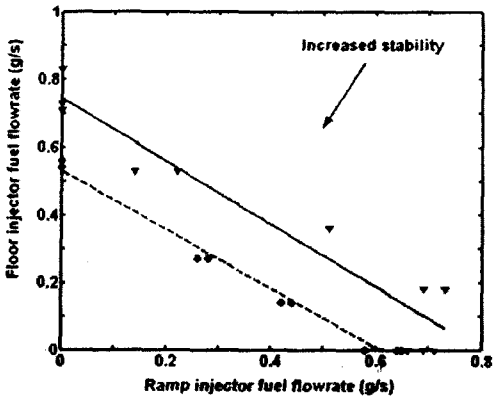

Figure 8: Lean blowout limits for simultaneous fuel injection of ethylene from both CR and CF injection locations at Mach 2 in the rectangular cavity. Two air flowrates were used, m^*_A=5.5 kg/s is marked with a ● and the dotted line and m^*_A=9.2 kg/s is denoted by ▼ and the solid line.

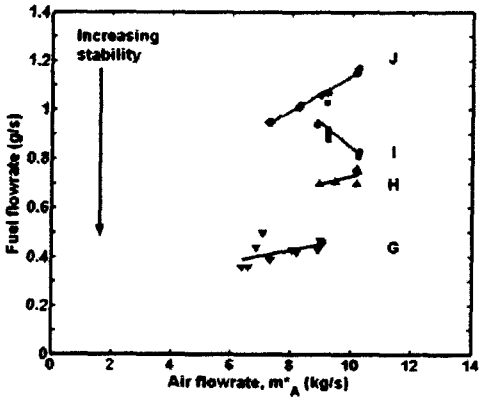

Figure 9: Lean blowout (LBO) limits for ethylene at Mach 3. The ramped cavity with CR injection offered the lowest stability limit. Curves show data for: G) ▼, CR injection, ramped cavity; H) ▲, CR injection, rectangular cavity; I) ■, CF injection, rectangular cavity; J) ●, CF injection, ramped cavity.

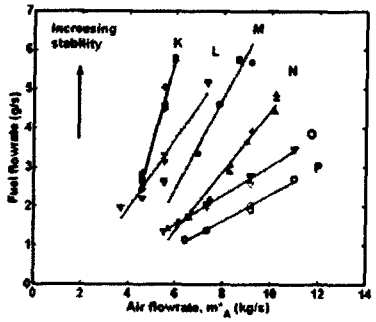

Figure 10: Rich blowout (RBO) limits for all conditions. Trends show similar slopes for all conditions. Methane curves blowout at the lowest limit followed by the Mach 3 ethylene cases and the Mach 2 ethylene cases give the highest limits. The only case with CF injection where upper blowout was reached was for ethylene in Mach 3, curve M. Conditions corresponding to the curves are: K) ●, Mach 2, ethylene, CR injection, ramped cavity; L) ▼, Mach 2, ethylene, CR injection, rectangular cavity; M) ■, Mach 3, ethylene, CF injection, ramped cavity; N) ▲, Mach 3, ethylene, CR injection, ramped cavity; O) ▽, Mach 2, methane, CR injection, rectangular cavity; P) O, Mach 2, methane, CR injection, ramped cavity.

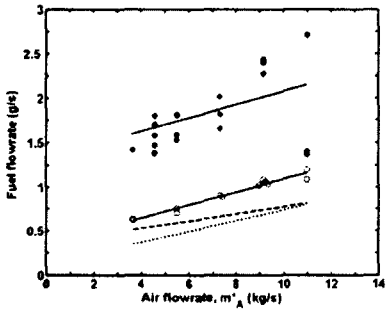

Figure 11: Fuel flowrates at ignition were much greater than at LBO. The above plot shows ignition and LBO fuel flowrates for a Mach 2 airflow with ethylene injected from the ramp. In the rectangular cavity, where ignition is symbolized by ● and the lean blowout by the dashed line, the ignition fuel flowrates were approximately 3 times the LBO value. In comparison, the ignition fuel flowrates were approximately 1.5 times higher than LBO in the ramped case, where ignition data denoted by O and LBO data by dotted line.

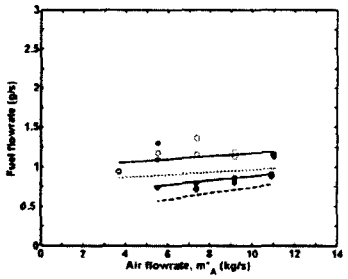

Figure 12: Ignition and LBO data are plotted above for ethylene in a Mach 2 airflow with CF injection. More fuel was required for ignition than at LBO and both phenomena exhibited similar dependence on m^*_A. The rectangular ignition is noted with a ● and the lean blowout is the dashed line, while the ignition data for the ramped cavity is indicated with a O and the LBO with a dotted line. In this case, the rectangular requires lower fuel flowrates at ignition and LBO.

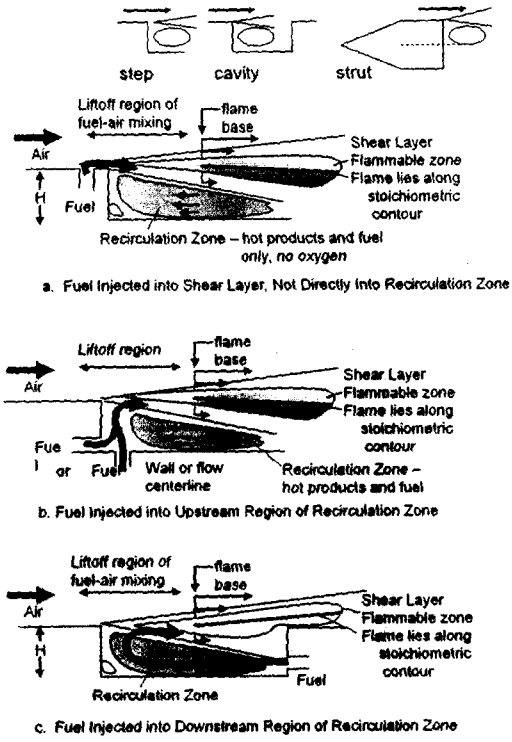

Figure 13. Schematic of Nonpremixed Flames Considered, Showing the Shear Layer Which Exists Between the Air Stream and the Recirculation Zone. Most of the reported bluff-body and swirl-stabilized flames are of type (b), strut fuel injectors are type (a), and cavity-stabilized geometries can be (a), (b) or (c).

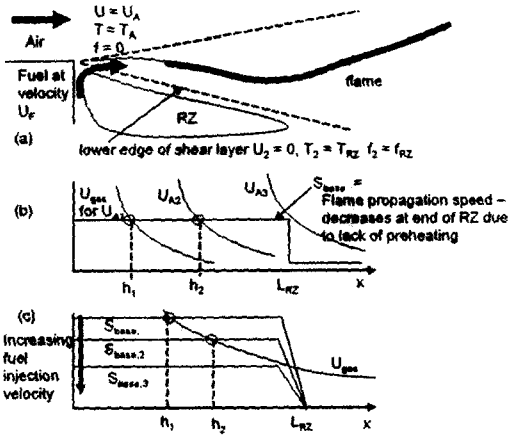

Figure 14. Schematic Diagrams Describing (a) the Stratified Shear Layer, (b) Lean Blowout due to Increasing the Air Velocity, and (c) Rich Blowout Due to Increasing the Fuel Flowrate. The gas velocity U_{gas} decreases in the x-direction along the stoichiometric contour; this curve shifts to the right in (b) due to increasing the air velocity U_A until the liftoff height h exceeds L_{RZ} and lean blowout occurs. In (c), increasing the fuel flowrate floods the recirculation zone with cold fuel and reduces both the RZ temperature and propagation speed S_{base} until the liftoff height h exceeds L_{RZ} and rich blowout occurs.